Relativistic many-body calculations of excitation energies and transition rates in ytterbiumlike ions

U. I. Safronova,* W. R. Johnson,† and M. S. Safronova‡
Department of Physics, 225 Nieuwland Science Hall, University of Notre Dame, Notre Dame, Indiana 46566

J. R. Albritton
Lawrence Livermore National Laboratory, P.O. Box 808, Livermore, California 94551
(Received 17 May 2002; published 27 August 2002)

Excitation energies, oscillator strengths, and transition rates are calculated for $(5d^2+5d6s+6s^2)-(5d6p+5d5f+6s6p)$ electric dipole transitions in Yb-like ions with nuclear charges Z ranging from 72 to 100. Relativistic many-body perturbation theory (RMBPT), including the retarded Breit interaction, is used to evaluate retarded $E1$ matrix elements in length and velocity forms. The calculations start from a $[\mathrm{Xe}]4f^{14}$ core Dirac-Fock potential. First-order RMBPT is used to obtain intermediate coupling coefficients, and second-order RMBPT is used to determine matrix elements. A detailed discussion of the various contributions to energy levels and dipole matrix elements is given for ytterbiumlike rhenium, $Z=75$. The resulting transition energies are compared with experimental values and with results from other recent calculations. Trends of excitation energies, line strengths, oscillator strengths, and transition rates as functions of nuclear charge Z are shown graphically for selected states and transitions. These calculations are presented as a theoretical benchmark for comparison with experiment and theory.

DOI: 10.1103/PhysRevA.66.022507 PACS number(s): 32.70.Cs, 31.15.Md, 31.25.Eb, 31.25.Jf

I. INTRODUCTION

We report results of *ab initio* calculations of excitation energies, oscillator strengths, and transition rates in Yb-like ions with nuclear charges Z ranging from 72 to 100. The ions considered here, starting from doubly ionized Hf III, all have $5d^2$ ground states. We do not consider Yb I and Lu II both of which have a $6s^2$ ground-state configuration. In recent publications [1–7], the spectra of Re VI, Os VII, and Ir VIII were studied and energies levels of the $5d^2$, $5d6s$, $5d6p$, $5d5f$, and $6s6p$ configurations were determined. The Cowan Hartree-Fock code [8] with relativistic and correlation options was used in Refs. [1–7] to calculate energy levels and to carry out least-squares adjustments of energies.

Although we do not consider Yb I and Lu II here, it should be noted that Porsev *et al.* [9] recently carried out elaborate calculations of electric-dipole amplitudes in atomic ytterbium. Moreover, Martin *et al.* [10] listed energies for 249 levels of Yb I and 40 levels of Lu II.

In the present paper, we use relativistic many-body perturbation theory (RMBPT) to determine energies of the 14 even-parity $5d^2$, $5d6s$, and $6s^2$ states and the 36 odd-parity $5d6p$, $5d5f$, and $6s6p$ states for Yb-like ions. We illustrate our calculation with a detailed study of Re VI, $Z=75$. Our first-order RMBPT calculations include both the Coulomb and retarded Breit interactions, but our second-order calculations are limited to the Coulomb interaction only.

Reduced matrix elements, line strengths, oscillator strengths, and transition rates are determined for all allowed and forbidden electric-dipole transitions between even-parity $(5d^2+5d6s+6s^2)$ and odd-parity $(5d6p+5d5f+6s6p)$ states. Retarded $E1$ matrix elements are evaluated in both length and velocity forms. RMBPT calculations that start from a local potential are gauge independent order-by-order, provided ''derivative terms'' are included in second- and higher-order matrix elements and careful attention is paid to negative-energy states. The present calculations start from a nonlocal $[\mathrm{Xe}]4f^{14}$ Dirac-Fock (DF) potential and consequently give gauge-dependent transition matrix elements. Second-order correlation corrections compensate almost exactly for the gauge dependence of the first-order matrix elements and lead to corrected matrix elements that differ by less than 5% in length and velocity forms for all of the ions considered here.

Energies from the present calculation agree well with results given in Refs. [1–7] for low-lying levels, but disagree substantially for various highly excited levels, as discussed later.

II. METHOD

The RMBPT formalism developed previously [11–15] for Be-, Mg-, and Ca-like ions is used here to describe perturbed wave functions, to obtain the second-order energies [11], and to evaluate first- and second-order transition matrix elements [13]. Ions of the Yb sequence, starting from the Hf III ion [16] and continuing onward have a $5d^2$ ground state. This is similar to the previously studied Ca sequence [15], where ions starting from Ti III have a $3d^2$ ground state. The primary differences between calculations for Ca-like and Yb-like ions arise from the increased number of the orbitals in the DF core potential, $[\mathrm{Xe}]4f^{14}$ instead of [Ar] ($[\mathrm{Ar}]=1s^22s^22p^63s^23p^6$ and $[\mathrm{Xe}]=[\mathrm{Ar}]3d^{10}4s^24p^64d^{10}5s^25p^6$), and the strong mixing be-

*Electronic address: usafrono@nd.edu
†Electronic address: johnson@nd.edu; URL: www.nd.edu/~johnson
‡Present address: Electron and Optical Physics Division, National Institute of Standards and Technology, Gaithersburg, MD 20899-8410; electronic address: msafrono@nd.edu

TABLE I. Possible two-particle states in the Yb-like ions.

jj coupling	*LS* coupling	*jj* coupling	*LS* coupling
$5d_{3/2}5d_{3/2}(0)$	$5d^2\,{}^3P_0$	$5d_{3/2}6p_{1/2}(2)$	$5d6p\,{}^3F_2$
$5d_{5/2}5d_{5/2}(0)$	$5d^2\,{}^1S_0$	$5d_{3/2}6p_{3/2}(2)$	$5d6p\,{}^3D_2$
$6s_{1/2}6s_{1/2}(0)$	$6s^2\,{}^1S_0$	$5d_{5/2}6p_{1/2}(2)$	$5d6p\,{}^1D_2$
		$5d_{5/2}6p_{3/2}(2)$	$5d6p\,{}^3P_2$
$5d_{3/2}5d_{5/2}(1)$	$5d^2\,{}^3P_1$	$5d_{3/2}5f_{5/2}(2)$	$6s6p\,{}^3P_2$
$5d_{3/2}6s_{1/2}(1)$	$5d6s\,{}^3D_1$	$5d_{3/2}5f_{7/2}(2)$	$5d5f\,{}^3F_2$
		$5d_{5/2}5f_{5/2}(2)$	$5d5f\,{}^1D_2$
$5d_{3/2}5d_{3/2}(2)$	$5d^2\,{}^3F_2$	$5d_{5/2}5f_{7/2}(2)$	$5d5f\,{}^3D_2$
$5d_{3/2}5d_{5/2}(2)$	$5d^2\,{}^1D_2$	$6s_{1/2}6p_{3/2}(2)$	$5d5f\,{}^3P_2$
$5d_{5/2}5d_{5/2}(2)$	$5d^2\,{}^3P_2$		
$5d_{3/2}6s_{1/2}(2)$	$5d6s\,{}^3D_2$	$5d_{3/2}6p_{3/2}(3)$	$5d6p\,{}^3F_3$
$5d_{5/2}6s_{1/2}(2)$	$5d6s\,{}^1D_2$	$5d_{5/2}6p_{1/2}(3)$	$5d6p\,{}^3D_3$
		$5d_{5/2}6p_{3/2}(3)$	$5d6p\,{}^1F_3$
$5d_{3/2}5d_{5/2}(3)$	$5d^2\,{}^3F_3$	$5d_{3/2}5f_{5/2}(3)$	$5d5f\,{}^3F_3$
$5d_{5/2}6s_{1/2}(3)$	$5d6s\,{}^3D_3$	$5d_{3/2}5f_{7/2}(3)$	$5d5f\,{}^3G_3$
		$5d_{5/2}5f_{5/2}(3)$	$5d5f\,{}^3D_3$
$5d_{3/2}5d_{5/2}(4)$	$5d^2\,{}^3F_4$	$5d_{5/2}5f_{7/2}(3)$	$5d5f\,{}^1F_3$
$5d_{5/2}5d_{5/2}(4)$	$5d^2\,{}^1G_4$		
		$5d_{5/2}6p_{3/2}(4)$	$5d6p\,{}^3F_4$
$5d_{3/2}6p_{3/2}(0)$	$5d6p\,{}^3P_0$	$5d_{3/2}5f_{5/2}(4)$	$5d5f\,{}^1G_4$
$5d_{5/2}5f_{5/2}(0)$	$6s6p\,{}^3P_0$	$5d_{3/2}5f_{7/2}(4)$	$5d5f\,{}^3H_4$
$6s_{1/2}6p_{1/2}(0)$	$5d5f\,{}^3P_0$	$5d_{5/2}5f_{5/2}(4)$	$5d5f\,{}^3F_4$
		$5d_{5/2}5f_{7/2}(4)$	$5d5f\,{}^3G_4$
$5d_{3/2}6p_{1/2}(1)$	$5d6p\,{}^3D_1$		
$5d_{3/2}6p_{3/2}(1)$	$5d6p\,{}^3P_1$	$5d_{3/2}5f_{7/2}(5)$	$5d5f\,{}^3H_5$
$5d_{5/2}6p_{3/2}(1)$	$5d6p\,{}^1P_1$	$5d_{5/2}5f_{5/2}(5)$	$5d5f\,{}^3G_5$
$5d_{3/2}5f_{5/2}(1)$	$6s6p\,{}^3P_1$	$5d_{5/2}5f_{7/2}(5)$	$5d5f\,{}^1H_5$
$5d_{5/2}5f_{5/2}(1)$	$5d5f\,{}^3D_1$		
$5d_{5/2}5f_{7/2}(1)$	$6s6p\,{}^1P_1$	$5d_{5/2}5f_{7/2}(6)$	$5d5f\,{}^3H_6$
$6s_{1/2}6p_{1/2}(1)$	$5d5f\,{}^3P_1$		
$6s_{1/2}6p_{3/2}(1)$	$5d5f\,{}^1P_1$		

tween both even-parity $(5d^2+5d6s+6s^2)$ and odd-parity $(5d6p+5d5f+6s6p)$ states. These differences lead to much more laborious numerical calculations. The calculations are carried out using sets of DF basis orbitals that are linear combinations of *B* splines. These *B*-spline basis orbitals are determined using the method described in Ref. [17]. We use 40 *B* splines of order 8 for each single-particle angular momentum state and we include all orbitals with orbital angular momentum $l \leqslant 7$ in our basis set.

A. Model space

The model spaces for the $(5d^2+5d6s+6s^2)$ and $(5d6p+5d5f+6s6p)$ complexes in Yb-like ions have 14 even-parity states and 36 odd-parity states, respectively. These states are summarized in Table I, where both *jj* and *LS* designations are given. When starting calculations from DF wave functions, it is natural to use *jj* designations for uncoupled matrix elements; however, neither *jj* nor *LS* coupling describes *physical* states properly, except for the single-configuration state $5d_{5/2}5f_{7/2}(6) \equiv 5d5f\,{}^3H_6$. The strong mixing between $5d6p$, $5d5f$, and $6s6p$ states was discussed previously in Refs. [1–7].

B. Example: Energy matrix for Re^{+5}

Details of the theoretical method used to evaluate second-order energies for ions with two valence electrons are given in Refs. [11,12] and will not be repeated here. The energy calculations are illustrated in Table II, where we list contributions to the energies of odd-parity $J=0$ states of Re^{+5}. We present zeroth-, first-, and second-order Coulomb energies $E^{(0)}, E^{(1)}$, and $E^{(2)}$ together with the first-order retarded Breit corrections $B^{(1)}$ [18]. It should be mentioned that the difference between first-order Breit corrections calculated with and without retardation is less than 2%. As one can see from Table II, the ratio of off-diagonal to diagonal matrix elements is larger for second-order contributions than for first-order contributions. Another difference between first- and second-order contributions concerns symmetry properties: first-order off-diagonal matrix elements are symmetric, whereas second-order off-diagonal matrix elements are unsymmetric [Lindgren and Morrison ([19], Chap. 9)]. Indeed, $E^{(2)}[Q,Q']$ and $E^{(2)}[Q',Q]$ differ in some cases by 20–50 % and occasionally even have opposite signs. The ratio of off-diagonal to diagonal matrix elements for Breit corrections $B^{(1)}$ is much smaller than for Coulomb corrections.

After evaluating the energy matrices, we calculate eigenvalues and eigenvectors for states with given values of *J* and parity. There are two possible methods to carry out the di-

TABLE II. Contributions to energy matrices $E[Q,Q']$ (a.u.) for odd-parity states $Q=n_1l_1j_1n_2l_2j_2(J)$, $Q'=n_3l_3j_3n_4l_4j_4(J)$ with $J=0$ before diagonalization in the case of Yb-like rhenium, $Z=75$.

Q,Q'	$E^{(0)}$	$E^{(1)}$	$B^{(1)}$	$E^{(2)}$
$5d_{3/2}6p_{3/2}, 5d_{3/2}6p_{3/2}$	−3.99398	0.427 31	0.006 79	−0.140 18
$5d_{5/2}5f_{5/2}, 5d_{5/2}5f_{5/2}$	−3.42978	0.448 89	0.004 30	−0.166 64
$6s_{1/2}6p_{1/2}, 6s_{1/2}6p_{1/2}$	−3.64181	0.297 37	0.005 91	−0.100 04
$5d_{3/2}6p_{3/2}, 5d_{5/2}5f_{5/2}$		−0.018 71	0.000 03	0.014 65
$5d_{5/2}5f_{5/2}, 5d_{3/2}6p_{3/2}$		−0.018 71	0.000 03	0.009 65
$5d_{3/2}6p_{3/2}, 6s_{1/2}6p_{1/2}$		0.021 91	−0.000 01	−0.012 78
$6s_{1/2}6p_{1/2}, 5d_{3/2}6p_{3/2}$		0.021 91	−0.000 01	−0.009 96
$5d_{5/2}5f_{5/2}, 6s_{1/2}6p_{1/2}$		−0.019 92	−0.000 01	0.002 21
$6s_{1/2}6p_{1/2}, 5d_{5/2}5f_{5/2}$		−0.019 92	−0.000 01	0.002 52

TABLE III. Energies of $5d^2$, $5d6s$, $6s^2$, $5d6p$, $5d5f$, and $6s6p$ states in Yb-like Re^{+5} (cm^{-1}). Notation: $E^{(0+1)}=E^{(0)}+E^{(1)}+B^{(1)}$.

Level	$E^{(0+1)}$	$E^{(2)}$	$E^{(\mathrm{tot})}$	$E^{(0+1)}$	$E^{(2)}$	$E^{(\mathrm{exc})}$
	Absolute energies			Excitation energies		
$5d^2\,^3F_2$	−1184 024	−40 817	−1224 841	0	0	0
$5d^2\,^3F_3$	−1177 178	−39 172	−1216 350	6847	1645	8491
$5d^2\,^3F_4$	−1170 966	−38 780	−1209 746	13 058	2037	15 095
$5d^2\,^3P_0$	−1167 037	−43 309	−1210 346	16 987	−2493	14 495
$5d^2\,^1D_2$	−1166 402	−41 572	−1207 975	17 622	−756	16 866
$5d^2\,^3P_1$	−1163 473	−41 812	−1205 285	20 551	−995	19 556
$5d^2\,^3P_2$	−1156 318	−40 152	−1196 470	27 706	665	28 371
$5d^2\,^1G_4$	−1155 966	−42 068	−1198 034	28 059	−1251	26 807
$5d^2\,^1S_0$	−1127 568	−46 217	−1173 785	56 456	−5400	51 056
$5d6s\,^3D_1$	−1097 044	−35 141	−1132 185	86 980	5675	92 656
$5d6s\,^3D_2$	−1094 845	−35 442	−1130 287	89 180	5375	94 554
$5d6s\,^3D_3$	−1087 729	−33 669	−1121 397	96 296	7148	103 444
$5d6s\,^1D_2$	−1079 142	−36 325	−1115 467	104 883	4491	109 374
$5d6p\,^3F_2$	−1030 357	−30 866	−1061 223	153 667	9951	163 618
$5d6p\,^3D_1$	−1024 847	−33 457	−1058 303	159 178	7360	166 538
$5d6p\,^3D_2$	−1018 155	−30 518	−1048 673	165 869	10 299	176 168
$5d6p\,^3F_3$	−1017 295	−30 334	−1047 629	166 729	10 483	177 212
$5d6p\,^1D_2$	−1012 677	−29 311	−1041 988	171 347	11 505	182 853
$5d6p\,^3D_3$	−1007 838	−30 332	−1038 169	176 187	10 485	186 672
$5d6p\,^3P_1$	−1005 870	−31 934	−1037 804	178 154	8882	187 037
$5d6p\,^3P_0$	−1004 380	−31 262	−1035 642	179 644	9554	189 199
$5d6p\,^3F_4$	−1001 386	−28 009	−1029 395	182 639	12 807	195 446
$5d6p\,^3P_2$	−999 246	−29 109	−1028 355	184 778	11 708	196 486
$5d6p\,^1F_3$	−995 855	−31 244	−1027 099	188 169	9573	197 742
$6s^2\,^1S_0$	−991 963	−34 225	−1026 189	192 061	6592	198 652
$5d6p\,^3P_1$	−989 455	−34 880	−1024 335	194 569	5936	200 506
$6s6p\,^3P_0$	−941 422	−21 782	−963 204	242 603	19 035	261 637
$6s6p\,^3P_1$	−936 597	−22 693	−959 291	247 427	18 123	265 550
$6s6p\,^3P_2$	−921 614	−21 582	−943 197	262 410	19 234	281 644
$5d5f\,^1G_4$	−914 890	−27 340	−942 229	269 135	13 477	282 611
$5d5f\,^3H_4$	−911 078	−28 960	−940 038	272 946	11 857	284 803
$5d5f\,^3H_5$	−910 564	−26 917	−937 481	273 460	13 900	287 360
$5d5f\,^3F_2$	−909 842	−32 013	−941 855	274 182	8804	282 986
$5d5f\,^3F_3$	−907 828	−33 638	−941 466	276 197	7178	283 375
$5d5f\,^3H_6$	−905 206	−23 491	−928 698	278 818	17 325	296 143
$5d5f\,^3F_4$	−903 304	−28 769	−932 074	280 720	12 047	292 767
$5d5f\,^1D_2$	−900 678	−34 598	−935 275	283 347	6219	289 565
$5d5f\,^3D_1$	−898 884	−36 856	−935 740	285 140	3960	289 100
$5d5f\,^3G_3$	−897 436	−41 168	−938 604	286 588	−352	286 237
$5d5f\,^3D_2$	−893 563	−36 014	−929 576	290 462	4803	295 265
$6s6p\,^1P_1$	−892 813	−36 571	−929 383	291 211	4246	295 457
$5d5f\,^3G_4$	−892 131	−38 708	−930 839	291 893	2108	294 002
$5d5f\,^3D_3$	−891 083	−38 081	−929 165	292 941	2735	295 676
$5d5f\,^3G_5$	−889 833	−39 291	−929 124	294 191	1526	295 717
$5d5f\,^3P_2$	−887 212	−36 551	−923 763	296 812	4266	301 078
$5d5f\,^3P_1$	−886 406	−36 865	−923 271	297 619	3952	301 570
$5d5f\,^3P_0$	−886 124	−36 385	−922 510	297 900	4431	302 331
$5d5f\,^1F_3$	−884 984	−39 786	−924 770	299 040	1031	300 071
$5d5f\,^1H_5$	−872 058	−49 224	−921 282	311 966	−8407	303 559
$5d5f\,^1P_1$	−866 971	−40 448	−907 419	317 054	369	317 422

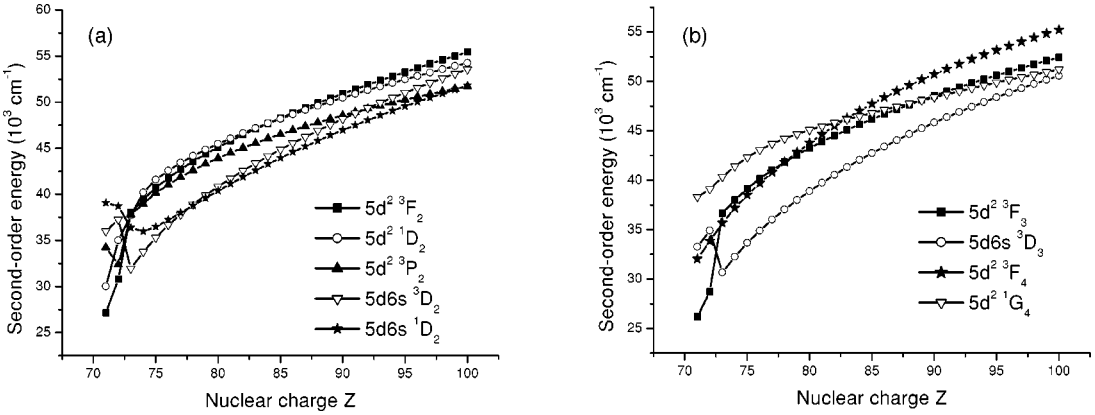

FIG. 1. Z dependence of the second-order energy $E^{(2)}$ for the $5d^2$ and $5d6s$ energy levels.

agonalization: either diagonalize the sum of zeroth- and first-order matrices, then calculate the second-order contributions using the resulting eigenvectors; or diagonalize the sum of the zeroth-, first- and second-order matrices together. Following Ref. [12], we choose the second method here.

The energy calculations are illustrated for Re^{+5} in Table III. Energies listed under the heading ''Absolute energies'' are given relative to the $[Xe]4f^{14}$ core, while those listed under the heading ''Excitation energies'' are given relative to the $5d^2\ ^3F_2$ ground state. In the table, we present absolute zeroth- plus first-order Coulomb and Breit energies $E^{(0+1)}=E^{(0)}+E^{(1)}+B^{(1)}$, absolute second-order Coulomb energies $E^{(2)}$, and the sum $E^{(\mathrm{tot})}$. We also give the breakdown of excitation energies and total excitation energies $E^{(\mathrm{exc})}$. As can be seen from the table, the second-order contribution is about 3% of the absolute energy but accounts for 5–15 % of the excitation energy. This table clearly illustrates the importance of including second-order contributions. As mentioned previously, neither jj nor LS coupling describes physical states properly; nevertheless, we use LS designations to label levels. We organize levels in the table according to decreasing values of $E^{(0+1)}$. After including second-order corrections, the present ordering differs in some cases from the ordering according to decreasing $E^{(\mathrm{tot})}$. Thus, the ordering of $5d^2\ ^3F_4$ and $5d^2\ ^3P_0$ levels, $5d5f\ ^3H_5$ and $5d5f\ ^3F_2$ levels, and $5d5f\ ^3G_4$ and $6s6p\ ^1P_1$ levels are interchanged in Re^{+5} after second-order corrections are added.

Problems arising when using different model spaces in RMBPT theory were examined by Johnson *et al.* [12]. A major difference between Yb-like and Be-like systems is that we could not construct as complete a model space for a two-electron system with a $[Xe]4f^{14}$ core as we did for a system with a [He] core [11]. To do so would require us to include all possible two-particle states that could be constructed from unoccupied $n=5$ and $n=6$ orbitals in our model space. In the case of Be-like ions, the model space is much simpler, being constructed from $n=2$ orbitals only. A second, but related, problem is that different model spaces lead to different results. For example, energy levels of Hg I, calculated using RMBPT with $(6s6p)$ and $(6s^2+6p^2)$ model spaces differ from those calculated with $(6s6p+6p6d)$ and $(6s^2+6p^2+6s6d)$ model spaces by about 500 cm^{-1} [12]. We confirm this result here comparing calculations of $5p6d$ energy levels starting from a $5p6d$ model space and those starting from $(5p6d+5d5f)$ or $(5p6d+5d5f+6s6p)$ model spaces in Re^{+5}. The largest difference occurs in the $E^{(2)}$, which changes by 1000 cm^{-1} in some cases. The change in $E^{(0+1)}$ is smaller by a factor of 2 and has an opposite sign. The resulting change in $E^{(\mathrm{tot})}$ is about 500 cm^{-1}. Similar tests of model-space dependence along the Yb sequence set a limit of about 500 cm^{-1} on the accuracy of the present second-order calculations.

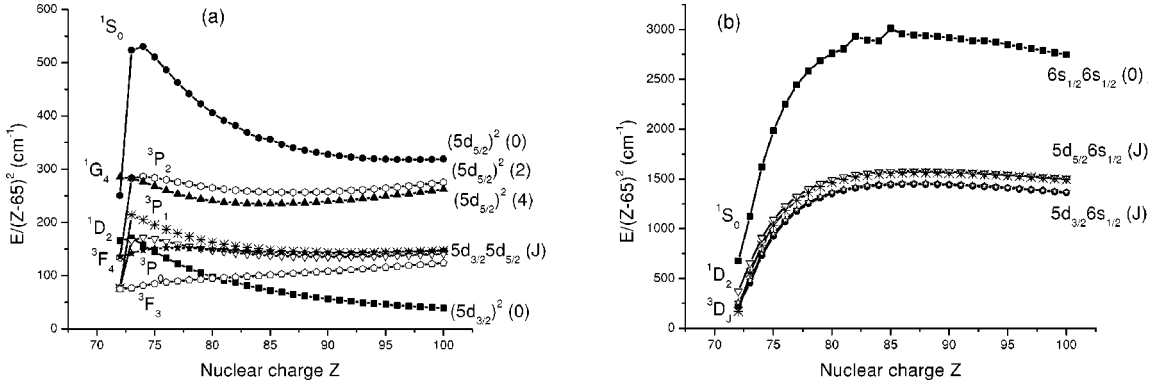

FIG. 2. Z dependence of the excitation energy $E^{(\mathrm{exc})}/(Z-65)^2$ in cm^{-1} for even-parity levels.

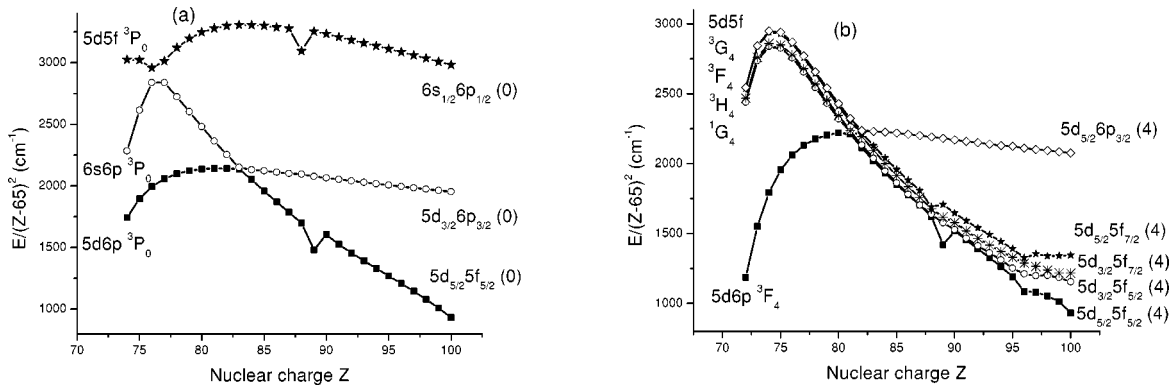

FIG. 3. Z dependence of the excitation energy $E^{(\mathrm{exc})}/(Z-65)^2$ in cm^{-1} for odd-parity levels.

C. Z dependence of energies

One unique feature of the present calculations is the inclusion of second-order correlation corrections. We illustrate the Z dependence of the second-order energy $E^{(2)}$ in Fig. 1 for even-parity levels with $J=2$ ($5d^2\,{}^3F_2$, ${}^1D_2$, ${}^3P_2$, and $5d6s\,{}^{1,3}D_2$) and $J=3,4$ ($5d^2\,{}^3F_3$, ${}^3F_4$, ${}^1G_4$, and $5d6s\,{}^3D_3$). As we can see from this figure, the second-order energy $E^{(2)}$ slowly increases with Z in the range $(3-5)\times10^4$ cm^{-1}. The smooth Z dependence for these nine terms is exceptional and is not found for other terms discussed below.

Excitation energies $E^{(\mathrm{exc})}$ of even-parity and odd-parity states relative to the $5d^2\,{}^3F_2$ ground state, divided by $(Z-65)^2$, are shown in Figs. 2 and 3. Both designations are shown in these figures: LS for low Z and jj for high Z. The variation of the $5d^2$ levels with Z is shown in Fig. 2(a). Strong mixing between $5d_{3/2}5d_{5/2}(J)$ and $5d_{5/2}5d_{5/2}(J)$ states with $J=2$ or 4 leads to rapid variations with Z in the corresponding Grotrian diagrams. Note that the ${}^1D_2$ and ${}^3F_4$ levels cross between $Z=79$ and 80, ${}^3P_0$ and ${}^3F_3$ levels cross between $Z=80$ and 81, and ${}^3P_1$ and ${}^3F_4$ levels cross between $Z=93$ and 94. We give excitation energies of the other five even-parity $5d6s$ and $6s^2$ levels in Fig. 2(b). Two small sharp features in the $6s^2$ level occur at $Z=82$ and $Z=85$. The origin of these irregularities is discussed in Appendix A. Energies of odd-parity levels with $J=0$ and 4, including the mixing of $5d6p$, $5d5f$, and $6s6p$ states, are given in Fig. 3. The sharp features in the curves describing $5d5f$ and $6s6p$ states are similar to those mentioned above for even-parity states and discussed in Appendix A. Avoided level crossings for the odd-parity $J=0$ levels are seen in Fig. 3(a) near $Z=76$ and $Z=84$. Similar avoided crossings can be observed for the odd-parity complex with $J=4$ in Fig. 3(b).

D. Z dependence of matrix elements for electric-dipole transitions

We designate the first-order dipole matrix element by $Z^{(1)}$, the Coulomb correction to the second-order matrix element by $Z^{(2)}$, and the second-order Breit correction by $B^{(2)}$. The evaluation of $Z^{(1)}$, $Z^{(2)}$, and $B^{(2)}$ for Yb-like ions follows the pattern of the corresponding calculation for berylliumlike ions in Refs. [13,20]. These matrix elements are calculated in both length and velocity gauges. Differences between length and velocity forms are illustrated for the uncoupled $5d_{3/2}5d_{5/2}(2)$-$5d_{5/2}6p_{1/2}(3)$ matrix element in Fig. 4. The second-order Breit matrix element $B^{(2)}$ is multiplied by a factor of 50 in order to put it on the same scale as the second-order Coulomb matrix element $Z^{(2)}$. The sharp features have the same origin as those in the the second-order energy matrix and are discussed in Appendix B. Contributions of the second-order matrix elements $Z^{(2)}$ and $B^{(2)}$ are much larger in velocity (V) form than in length (L) form as seen in panels (a) and (b) of Fig. 4. As shown later, L-V differences are compensated by "derivative terms" $P^{(\mathrm{derv})}$.

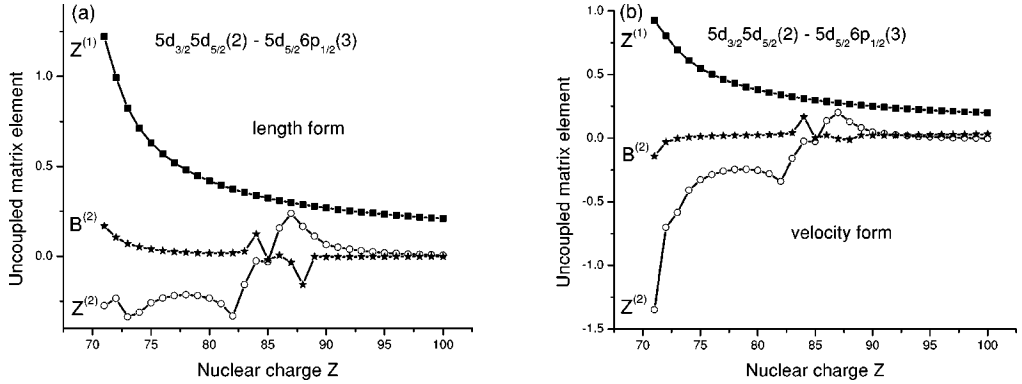

FIG. 4. Uncoupled matrix elements for the $5d_{3/2}5d_{5/2}(2)$-$5d_{5/2}6p_{1/2}(3)$ transition calculated in velocity and length forms.

TABLE IV. Uncoupled reduced matrix elements in length L and velocity V forms for even-odd parity transitions in Re^{+5}.

Even-parity	Odd-parity	$Z_L^{(1)}$	$Z_V^{(1)}$	$Z_L^{(2)}$	$Z_V^{(2)}$	$B_L^{(2)}$	$B_V^{(2)}$	$P_L^{(\mathrm{derv})}$	$P_V^{(\mathrm{derv})}$
$5d_{3/2}5d_{3/2}(0)$	$5d_{3/2}6p_{1/2}(1)$	0.847 36	0.737 95	−0.181 76	−0.322 01	0.001 05	0.000 32	0.847 33	−0.000 01
$5d_{3/2}5d_{3/2}(0)$	$5d_{3/2}6p_{3/2}(1)$	−0.335 05	−0.292 06	0.006 33	0.039 76	−0.000 74	−0.000 53	−0.335 02	0.000 03
$5d_{3/2}5d_{3/2}(0)$	$5d_{5/2}6p_{3/2}(1)$	0.000 00	0.000 00	−0.064 16	−0.099 97	0.000 02	0.000 00	0.000 00	0.000 00
$5d_{5/2}5d_{5/2}(0)$	$5d_{3/2}6p_{1/2}(1)$	0.000 00	0.000 00	−0.040 75	−0.084 23	−0.000 01	−0.000 02	0.000 00	0.000 00
$5d_{5/2}5d_{5/2}(0)$	$5d_{3/2}6p_{3/2}(1)$	0.000 00	0.000 00	0.050 57	0.075 83	0.000 00	0.000 01	0.000 00	0.000 00
$5d_{5/2}5d_{5/2}(0)$	$5d_{5/2}6p_{3/2}(1)$	0.870 30	0.750 77	−0.150 75	−0.262 97	0.001 00	0.000 55	0.870 28	0.000 03
$6s_{1/2}6s_{1/2}(0)$	$5d_{3/2}6p_{1/2}(1)$	0.000 00	0.000 00	−0.301 43	0.036 09	0.000 06	0.000 04	0.000 00	0.000 00
$6s_{1/2}6s_{1/2}(0)$	$5d_{3/2}6p_{3/2}(1)$	0.000 00	0.000 00	0.201 41	−0.187 19	−0.000 03	−0.000 01	0.000 00	0.000 00
$6s_{1/2}6s_{1/2}(0)$	$5d_{5/2}6p_{3/2}(1)$	0.000 00	0.000 00	−0.535 34	0.909 41	0.000 06	0.000 11	0.000 00	0.000 00

E. Example: Dipole matrix elements in Re^{+5}

We list uncoupled first- and second-order dipole matrix elements $Z^{(1)}, Z^{(2)}, B^{(2)}$, together with derivative terms $P^{(\mathrm{derv})}$ for Re^{+5} in Table IV. For simplicity, we consider only the nine dipole transitions between even-parity states with $J=0$ and odd-parity states with $J=1$. The derivative terms shown in Table IV arise because transition amplitudes depend on energy, and the transition energy changes order-by-order in perturbation theory. Both L and V forms are given for the matrix elements. We see that the first-order matrix elements $Z_L^{(1)}$ and $Z_V^{(1)}$ differ by 10–20 % and that the L-V differences between second-order matrix elements are much larger for some transitions. The first-order matrix elements $Z_L^{(1)}$ and $Z_V^{(1)}$ are nonzero for the three matrix elements $5d_{3/2}5d_{3/2}(0)$-$5d_{3/2}6p_{1/2}(1)$, $5d_{3/2}5d_{3/2}(0)$-$5d_{3/2}6p_{3/2}(1)$, and $5d_{5/2}5d_{5/2}(0)$-$5d_{5/2}6p_{3/2}(1)$, but vanish for the remaining six transitions. Moreover, for those six transitions, $Z_L^{(2)}$ and $Z_V^{(2)}$ have the same order of magnitude as the three nonzero first-order matrix elements. This confirms the importance of including higher-order RMBPT corrections. It can also be seen from Table IV that $P_L^{(\mathrm{derv})}$ is almost equal to $Z_L^{(1)}$ but $P_V^{(\mathrm{derv})}$ is smaller than $Z_V^{(1)}$ by five to six orders of magnitude.

In Table V, line strengths for Re^{+5} in length and velocity forms are given for the $J=0$–$J'=1$ transitions considered in Table IV as well as for other J-J' transitions. We see that L and V forms of the coupled matrix elements in Table V differ only in the second or third digits. As mentioned in the Introduction, these L-V differences arise because we start our RMBPT calculations using a nonlocal DF potential. If we were to replace the DF potential by a local potential, the differences would disappear completely. Another source of L-V differences is the incomplete model space. The last two columns in Table V show L and V values of line strengths calculated without the second-order contribution. As can be seen, including second-order corrections significantly decreases L-V differences.

TABLE V. Line strengths in length L and velocity V forms for even-odd-parity transitions in Re^{+5}.

		RMBPT		First order	
Level	Level	L	V	L	V
$5d^2\,{}^3P_0$	$5d6p\,{}^3D_1$	0.2632	0.2312	0.4952	0.3749
$5d^2\,{}^3P_0$	$5d6p\,{}^3P_1$	0.2424	0.2277	0.2673	0.2027
$5d^2\,{}^3P_0$	$5d6p\,{}^1P_1$	0.0645	0.0651	0.0532	0.0391
$5d^2\,{}^1S_0$	$5d6p\,{}^3D_1$	0.0040	0.0032	0.0375	0.0288
$5d^2\,{}^1S_0$	$5d6p\,{}^3P_1$	0.0050	0.0052	0.0272	0.0208
$5d^2\,{}^1S_0$	$5d6p\,{}^1P_1$	0.3261	0.3437	0.7024	0.5236
$5d^2\,{}^3P_1$	$5d6p\,{}^3P_0$	0.5035	0.5010	0.5657	0.4208
$5d6s\,{}^3D_1$	$5d6p\,{}^3P_0$	1.1657	1.1792	1.6949	1.5356
$5d^2\,{}^3P_1$	$5d6p\,{}^3D_1$	0.0080	0.0081	0.0242	0.0179
$5d^2\,{}^3P_1$	$5d6p\,{}^3P_1$	0.4143	0.4127	0.5065	0.3774
$5d^2\,{}^3P_1$	$5d6p\,{}^1P_1$	0.0358	0.0340	0.0346	0.0264
$5d6s\,{}^3D_1$	$5d6p\,{}^3P_1$	2.1855	2.2762	3.0478	2.7590
$5d^2\,{}^3P_1$	$5d6p\,{}^1D_2$	0.0274	0.0296	0.0709	0.0528
$5d^2\,{}^3P_1$	$5d6p\,{}^3P_2$	0.2803	0.2573	0.2959	0.2251
$5d^2\,{}^3F_2$	$5d6p\,{}^3P_1$	0.1648	0.1639	0.1486	0.1122
$5d^2\,{}^3F_2$	$5d6p\,{}^3D_2$	0.1145	0.1145	0.1690	0.1262
$5d6s\,{}^3D_2$	$5d6p\,{}^3P_2$	1.2140	1.2595	1.5450	1.3925
$5d^2\,{}^1D_2$	$5d6p\,{}^3F_3$	0.0380	0.0361	0.1735	0.1284
$5d6s\,{}^3D_2$	$5d6p\,{}^3F_3$	2.4488	2.7097	3.3267	3.0271
$5d^2\,{}^3F_3$	$5d6p\,{}^1D_2$	1.6146	1.6111	1.7279	1.2837
$5d^2\,{}^3F_3$	$5d6p\,{}^3P_2$	0.1384	0.1440	0.1441	0.1079
$5d6s\,{}^3D_3$	$5d6p\,{}^3F_2$	0.0020	0.0027	0.0026	0.0024
$5d6s\,{}^3D_3$	$5d6p\,{}^3P_2$	2.7197	2.9674	3.8172	3.4676
$5d^2\,{}^3F_3$	$5d6p\,{}^3F_3$	1.6878	1.5330	1.9319	1.4599
$5d^2\,{}^3F_3$	$5d6p\,{}^3D_3$	0.0528	0.0563	0.0308	0.0219
$5d6s\,{}^3D_3$	$5d6p\,{}^1F_3$	1.7322	1.8326	2.3084	2.0843
$5d^2\,{}^3F_3$	$5d6p\,{}^3F_4$	0.1367	0.1294	0.1291	0.0983
$5d6s\,{}^3D_3$	$5d6p\,{}^3F_4$	11.1345	11.5018	15.2305	13.8004
$5d^2\,{}^3F_4$	$5d6p\,{}^3F_3$	0.5896	0.5200	0.8001	0.6090
$5d^2\,{}^3F_4$	$5d6p\,{}^3D_3$	3.6963	3.6447	4.0769	3.0379
$5d^2\,{}^3F_4$	$5d6p\,{}^1F_3$	0.1442	0.1561	0.1513	0.1095
$5d^2\,{}^1G_4$	$5d6p\,{}^3D_3$	0.3118	0.3027	0.3497	0.2616
$5d^2\,{}^1G_4$	$5d6p\,{}^1F_3$	5.6434	5.5815	6.2102	4.6443
$5d^2\,{}^3F_4$	$5d6p\,{}^3F_4$	1.9537	1.9011	1.9296	1.4447
$5d^2\,{}^1G_4$	$5d6p\,{}^3F_4$	0.1544	0.1571	0.1535	0.1114

III. RESULTS AND DISCUSSION

We calculate energies of the 14 even-parity $5d^2$, $5d6s$, and $6s^2$ states as well as the 36 odd-parity $5d6p$, $5d5f$, and

TABLE VI. Energy levels (cm^{-1}) in ytterbium isoelectronic sequence. Comparison of RMBPT results with experimental data presented in Refs. [1–5].

Level	Re VI		Os VII		Ir VIII		Pt IX		Au X		Hg XI	
	RMBPT	[1]	RMBPT	[2,3]	RMBPT	[2,3]	RMBPT	[4]	RMBPT	[5]	RMBPT	[5]
$5d^2\,^3F_2$	0	0	0	0	0	0	0	0	0	0	0	0
$5d^2\,^3F_3$	8491	8167	10 604	10 308	12 932	12 672	15 490	15 250	18 284	18 077	21 325	21 175
$5d^2\,^3P_0$	14 495	14 379	16 117	15 837	17 670	17 254	19 174	18 612	20 638	19 949	22 055	21 255
$5d^2\,^3F_4$	15 095	14 679	18 409	18 049	21 920	21 615	25 633	25 359	29 550	29 309	33 677	33 481
$5d^2\,^1D_2$	16 866	16 577	19 852	19 444	22 905	22 436	26 146	25 568	29 568	28 925	33 211	32 513
$5d^2\,^3P_1$	19 556	19 142	22 624	22 098	25 841	25 222	29 238	28 515	32 832	32 039	36 643	35 802
$5d^2\,^1G_4$	26 807	26 657	31 496	31 274	36 522	36 253	41 949	41 610	47 818	47 451	54 165	53 918
$5d^2\,^3P_2$	28 371	27 723	33 932	33 127	39 735	38 878	45 962	44 991	52 588	51 566	59 691	58 835
$5d^2\,^1S_0$	51 056	50 492	58 851	57 710	66 656	65 022	74 624	72 527	82 848	80 385	91 380	88 897
$5d6s\,^3D_1$	92 656	92 312	129 438	129 244	169 138	169 223	211 579		256 622		304 159	
$5d6s\,^3D_2$	94 554	94 262	131 488	131 416	171 413	171 485	214 009		259 236		306 918	
$5d6s\,^1D_2$	109 374	108 709	148 595	148 023	191 018	190 553	236 412		284 633		335 596	
$5d6s\,^3D_3$	103 444	102 712	142 679	142 163	185 041	184 748	230 364		278 518		329 409	
$6s^2\,^1S_0$	198 652		272 504	282 345	352 159	363 633	437 184		527 172		621 600	
$5d6p\,^3F_2$	163 618	162 134	209 906	208 659	259 044	258 017	310 888	310 064	365 322	364 711	422 250	422 506
$5d6p\,^3D_1$	166 538	166 077	213 084	212 862	262 439	262 461	314 456	314 751	369 016	369 624	426 038	426 672
$5d6p\,^3D_2$	176 168	174 761	224 886	223 453	276 670	275 872	331 369	330 850	388 865	388 660	449 056	449 335
$5d6p\,^3F_3$	177 212	175 502	226 212	224 741	278 237	276 994	333 148	332 117	390 829	390 038	451 183	450 786
$5d6p\,^1D_2$	182 853	181 154	233 874	232 453	288 280	287 122	345 942	345 026	406 770	406 109	470 688	470 408
$5d6p\,^3D_3$	186 672	185 022	238 186	236 726	293 068	291 792	351 186	350 075	412 435	411 533	476 719	476 134
$5d6p\,^3P_1$	187 037	185 963	238 656	237 682	293 545	292 734	351 634	350 986	412 843	412 413	477 109	476 749
$5d6p\,^3P_0$	189 199	187 780	241 043	239 794	296 204	295 142	354 580	353 689	416 091		480 682	480 075
$5d6p\,^3F_4$	195 446	193 260	249 334	247 354	306 792	305 005	367 714	366 087	432 023	430 576	499 662	498 310
$5d6p\,^3P_2$	196 486	194 539	250 142	248 453	307 362	305 894	368 050	366 803	432 129	431 126	499 533	498 771
$5d6p\,^1F_3$	197 742	195 691	251 254	249 401	308 315	306 697	368 814	367 435	432 644	431 579	499 643	499 109
$5d6p\,^1P_1$	200 506	200 437	255 391	255 246	313 586	313 520	375 052	375 145	439 684	440 120	507 190	508 193
$6s6p\,^3P_0$	261 637		343 490		408 884		460 493	456 143	510 225		558 566	
$6s6p\,^3P_1$	265 550		341 677	341 844	394 150	391 888	443 224	438 038	490 445		536 100	
$6s6p\,^3P_2$	281 644	279 156	333 322	332 501	381 777	379 116	428 519	424 403	473 776		517 742	
$5d5f\,^1G_4$	282 611	280 575	333 410	331 454	382 478	380 334	430 103	425 349	476 544		522 022	
$5d5f\,^3F_2$	282 986	281 906	341 072	340 330	391 578	388 229	440 422	435 302	487 930		534 343	
$5d5f\,^3F_3$	283 375	283 559	334 390	334 240	383 305	380 724	430 253	422 093	475 351		518 717	
$5d5f\,^3H_4$	284 803	282 853	336 142	334 302	385 817	383 508	434 072	430 412	481 126		527 163	
$5d5f\,^3G_3$	286 237	286 426	338 249	337 436	388 358	385 282	436 878	425 627	484 128		530 397	
$5d5f\,^3H_5$	287 360	285 346	339 706	337 535	390 378	387 545	439 680	436 230	487 868		535 150	
$5d5f\,^3D_1$	289 100	290 208	349 008		408 218	406 542	459 678	456 053	509 418		557 828	
$5d5f\,^1D_2$	289 565	288 853	348 392	347 386	399 983	397 557	449 925	442 048	498 451		545 750	
$5d5f\,^3F_4$	292 767	290 824	345 648	343 897	396 931	393 669	446 783	439 406	495 294		542 569	
$5d5f\,^3G_4$	294 002	293 741	347 287	346 144	398 865	396 001	449 051	445 365	498 219		546 694	
$5d5f\,^3D_2$	295 265	294 688	354 838	354 012	408 411	405 867	460 122	456 798	510 546		559 987	
$6s6p\,^1P_1$	295 457		357 819	356 849	420 585	421 774	477 574		532 630		586 680	
$5d5f\,^3D_3$	295 676	295 836	349 683	349 155	401 804	397 003	452 259	436 157	501 264		549 026	
$5d5f\,^3G_5$	295 717	295 928	349 829	349 324	402 320	399 128	453 392	443 691	503 255		552 106	
$5d5f\,^3H_6$	296 143	292 600	349 940		402 394		453 792		504 385		554 394	
$5d5f\,^1F_3$	300 071	300 794	356 198	356 322	410 808	408 418	464 085	461 735	516 269		567 655	
$5d5f\,^3P_2$	301 078	301 178	371 823		465 428		565 480		671 378		782 904	
$5d5f\,^3P_1$	301 570	302 600	362 544	363 927	440 737		534 533		634 090		738 793	
$5d5f\,^3P_0$	302 331	303 600	358 117	356 587	434 121		527 597		626 622		730 708	
$5d5f\,^1H_5$	303 559	307 440	361 850	364 949	418 559	420 291	473 757	470 214	527 612		580 323	
$5d5f\,^1P_2$	317 422	317 600	396 700		489 065		589 085		695 429		807 602	

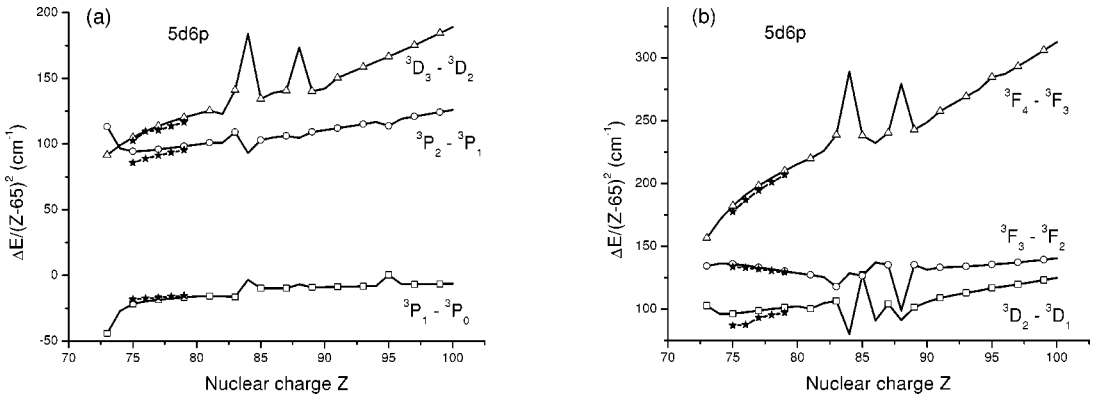

FIG. 5. Fine-structure intervals $\Delta E/(Z-65)^2$ in cm^{-1} of $5d6p\ ^3P$, $5d6p\ ^3D$, and $5d6p\ ^3F$ terms as a function of Z. Experimental data represented by the * symbol are from [1–7].

$6s6p$ states for Yb-like ions with nuclear charges in the range $Z=72$ to 100. Reduced matrix elements, line strengths, oscillator strengths, and transition rates are also determined for all electric-dipole transitions between even-parity and odd-parity states for each ion. Comparisons with experimental data and other theoretical results are also given. Our results are presented in three parts: transition energies, fine-structure energy differences, and trends of line strengths, oscillator strengths, and transition rates.

A. Transition energies

In Table VI, transition energies are compared with recent measurements [1–7]. We obtain good agreement with the experiment for low-lying $5d^2$, $5d6s$, and $5d6p$ levels. We also obtain reasonable agreement (500–1000 cm^{-1}) for highly excited $5d5f$ levels in Re VI, Os VII, and Ir VIII ions. However, we disagree substantially (2000–10 000 cm^{-1}) for $5d5f$ levels in Pt IX, Au X, and Hg XI ions. As mentioned in Refs. [4–6], mixing between levels of the $5d5f$ configuration and the core excited configurations with a $5p$ hole could be very important for Pt IX, Au X, and Hg XI ions. Indeed, substantial mixing of the $5p^55d^3$ and $5p^65d5f$ configurations was found in Ref. [6]. From this, we conclude that the present values for $5d5f$ configurations in Pt IX, Au X, and Hg XI are less reliable ($\sim$1%) than data for Re VI, Os VII, and Ir VIII.

B. Fine structure of the $5d6p$ triplets

The fine-structure intervals for the ^3P, ^3D, and ^3F terms of the $5d6p$ configuration divided by $(Z-65)^2$ are shown in Fig. 5. The fine structures of these levels do not follow the Landé rules even for small Z; the ^3P levels are partially inverted, while the ^3D and ^3F levels show regular ordering of the fine-structure splittings for both low and high Z. The unusual splittings are caused by changes from LS to jj coupling and by mixing from other triplet and singlet states. Comparisons are made with experimental data from [1–7] in Fig. 5. Excellent agreement (0.3–3 %) is found for the four intervals $^3P_1$-$^3P_0$, $^3D_3$-$^3D_2$, $^3F_4$-$^3F_3$, and $^3F_3$-$^3F_2$. The agreement improves for the $^3P_2$-$^3P_1$ and $^3D_2$-$^3D_1$ intervals, from 10% for Re^{+5} to 2% for Hg^{+10}. Experimental energies for other ions would be very helpful in confirming the Z dependence shown in Fig. 5.

C. Line strengths and oscillator strengths in Yb-like ions

Trends of the Z dependence of line strengths and oscillator strengths are shown in Figs. 6 and 7. In Fig. 6, we illustrate the Z dependence of line strengths for the four $5d^2$-$5d6p$ transitions calculated (a) by RMBPT and (b) in first order to illustrate once again the importance of including second-order matrix elements. Comparing the curves in Figs. 6(a) and 6(b), we can see that the Z dependence is the same

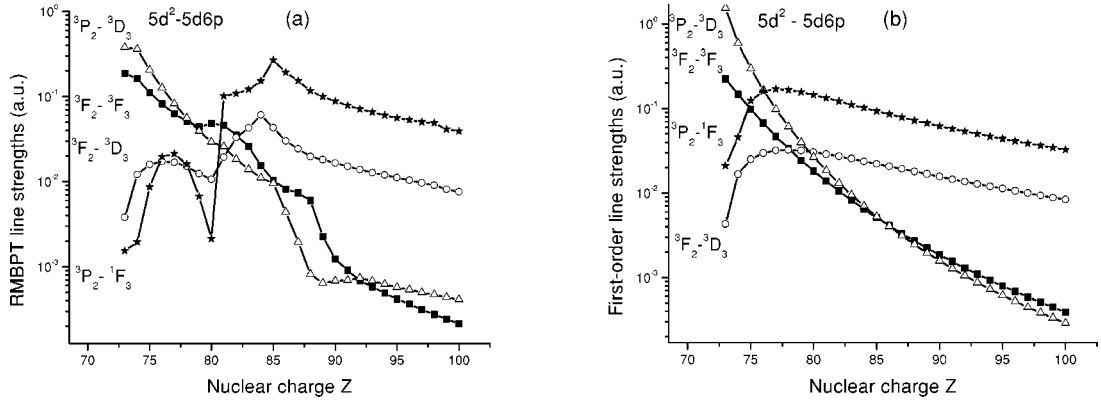

FIG. 6. Line strengths for $5d^2$-$5d6p$ transitions in Yb-like ions: (a) RMBPT; (b) first-order approximation.

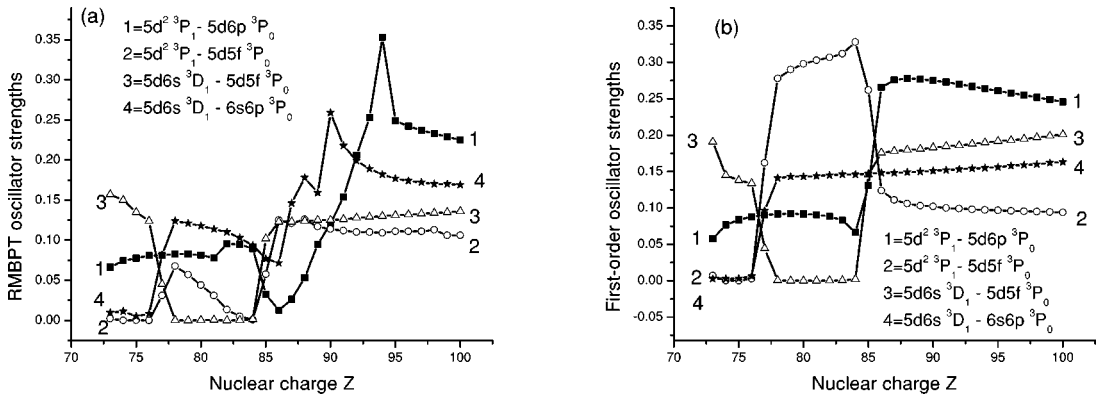

FIG. 7. Oscillator strengths for transitions from even-parity complex with $J=1$ to odd-parity complex with $J=0$ in Yb-like ions: (a) RMBPT; (b) first-order approximation.

for both cases except for the small region $Z=80$–88. The singularities in this region are already present for uncoupled dipole matrix elements. The second-order contribution for the $5d_{3/2}5d_{5/2}(2)$-$5d_{5/2}6p_{1/2}(3)$ uncoupled matrix element is shown in Fig. 4. Similar singularities appear for other uncoupled matrix elements between even-parity $J=2$ states and odd-parity $J=3$ states. Consequently, those singularities also appear in the coupled matrix elements and the line strengths shown in Fig. 6.

The Z dependence is more complicated for transitions between even-parity states with $J=1$ and odd-parity states with $J=0$, as seen in Fig. 7, where we give oscillator strengths for four transitions calculated (a) by RMBPT and (b) in first order. The oscillator strength curves are not smooth functions of Z, even in first order. The singularities shown in the four curves of Fig. 7(b) arise from the strong mixing between three states of the odd-parity complex with $J=0$. The mixing of $5d_{5/2}5d_{5/2}$, $5d_{3/2}6p_{3/2}$, and $6s_{1/2}6p_{1/2}$ states was discussed earlier in Fig. 3(a) where it was shown that avoided crossings occur near $Z=76$ and 84.

IV. CONCLUSION

In summary, a systematic second-order RMBPT study of the energies of the $5d^2$, $5d6s$, $6s^2$, $5d6p$, $5d5f$, and $6s6p$ states of Yb-like ions has been presented. These calculations agree with existing experimental energy data for intermediate $Z=75$ to 80 at the level of 500–1000 cm^{-1} for low-lying $5d^2$, $5d6s$, and $5d6p$ levels. They provide a smooth theoretical reference database for the identification of lines.

Also presented is a systematic second-order relativistic RMBPT study of reduced matrix elements, line strengths, oscillator strengths, and transition rates for allowed and forbidden electric-dipole transitions in Yb-like ions with nuclear charges ranging from $Z=72$ to 100. The dipole matrix elements include retardation and correlation corrections from Coulomb and Breit interactions. Both length and velocity forms of the matrix elements are evaluated, and $\sim 5\%$ differences, caused by the nonlocality of the starting DF potential, are found between the two forms.

We believe that our results will be useful in analyzing existing experimental data and planning new experiments. There remains a paucity of experimental data for many of the higher ionized members of this sequence, both for term energies and for transition probabilities and lifetimes. Additionally, matrix elements from the present calculations will provide basic theoretical input for calculations of reduced matrix elements, oscillator strengths, and transition rates in three-electron Lu-like ions.

ACKNOWLEDGMENTS

The work of W.R.J. and M.S.S. was supported in part by National Science Foundation Grant No. PHY-01-39928. U.I.S. acknowledges partial support by Grant No. B516165 from Lawrence Livermore National Laboratory. The work of J.R.A was performed under the auspices of the U. S. Department of Energy by the University of California, Lawrence Livermore National Laboratory under Contract No. W-7405-Eng-48. We also acknowledge helpful discussions with Professor A. N. Ryabtsev.

APPENDIX A: SECOND-ORDER DOUBLE-EXCITATION CONTRIBUTION

Here, we consider second-order double-excitation contribution to explain singularities in the Z dependence of energy levels given in Figs. 2 and 3. A typical contribution from one of the double-excitation diagrams for the second-order interaction energy has the form [11]

$$A_l(vw;v'w') \propto \sum_{mn} \sum_{kk'} \frac{X_k(vwmn)X_{k'}(mnv'w')}{\epsilon_{v'}+\epsilon_{w'}-\epsilon_m-\epsilon_n}, \tag{A1}$$

where $X_{k'}(vwmn)$ are products of angular coupling coefficients and Slater integrals [11], ϵ_m is the single-particle energy for state m, and v designates a single-particle valence state $(n_v l_v j_v)$. For the case of a $[\mathrm{Xe}]4f^{14}$ core, sums over m and n include $5d_{3/2}, 5d_{5/2}, 5f_{5/2}, 5f_{7/2}, 5g_{7/2}, 5g_{9/2}$, and all states with principal quantum number $n>5$. We must, however, exclude terms with pairs (mn) that are included in model space. Therefore, we remove the pairs $(5d5d)$, $(5d6s)$, and $(6s6s)$ since they are in the even-parity model space and pairs $(5d6p)$, $(5d5f)$, and $(6s6p)$ in the odd-parity model space.

As an example, let us consider the singularity near $Z=85$ in the curve describing the energy of the $6s^2$ level in Fig. 2(b). The denominator in Eq. (A1) is $D=2\epsilon_{6s}-\epsilon_m-\epsilon_n$ for the matrix element $A_I(6s_{1/2}6s_{1/2};6s_{1/2}6s_{1/2})$. For an ion with $Z=85$, D becomes very small when $(mn)=(5d_{3/2}6d_{3/2})$ since $\epsilon_{6s_{1/2}}=-9.488\,404$ a.u., $\epsilon_{5d_{3/2}}=-12.069\,226$ a.u., and $\epsilon_{6d_{3/2}}=-6.932\,272$ a.u., giving $D=0.024\,69$. This one term dominates the matrix element $A_I(6s_{1/2}6s_{1/2};6s_{1/2}6s_{1/2})$ and increases its size by a factor of 6 in comparison with values for neighboring Z, explaining the singularity at $Z=85$ in Fig. 2(b). The explanation of the sharp features in the curves describing energies of the $6s_{1/2}6p_{1/2}$ and $5d_{5/2}5f_{5/2}$ levels in Fig. 3 is similar.

APPENDIX B: SECOND-ORDER DIPOLE MATRIX ELEMENT

A typical contribution from one of the second-order correlation corrections to the dipole matrix element $[vw(J)-v'w'(J')]$ has the form [13]

$$Z^{(\mathrm{corr})}[vw(J)-v'w'(J')]\propto\sum_i\frac{Z_{iv}X_k(v'w'wi)}{\epsilon_i+\epsilon_w-\epsilon_{v'}-\epsilon_{w'}},$$

where Z_{iv} is a single-electron dipole matrix element. In the sum over i, only terms with vanishing denominators are excluded. For the $5d_{5/2}5d_{3/2}(2)$-$5d_{5/2}6p_{1/2}(3)$ transition, we obtain

$$Z^{(\mathrm{corr})}[5d_{5/2}5d_{3/2}(2)-5d_{5/2}6p_{1/2}(1)]\propto\sum_i\frac{Z(i,5d_{5/2})X_k(5d_{5/2}6p_{1/2}5d_{3/2}i)}{\epsilon_i+\epsilon(5d_{3/2})-\epsilon(5d_{5/2})-\epsilon(6p_{1/2})}.$$

For the case $i=5f_{7/2}$ and $Z=84$, the denominator becomes

$$\epsilon_i+\epsilon(5d_{3/2})-\epsilon(5d_{5/2})-\epsilon(6p_{1/2})=0.003.$$

This one term dominates the entire matrix element. For the $5d_{5/2}5d_{5/2}(0)$-$5d_{3/2}6p_{1/2}(1)$ transition, the denominator becomes very small at $Z=88$ when $i=5f_{7/2}$:

$$\epsilon_i+\epsilon(5d_{5/2})-\epsilon(5d_{3/2})-\epsilon(6p_{1/2})=-0.056.$$

Again, this single term dominates the matrix element.

A typical contribution from the second-order random-phase approximation (RPA) correction for dipole matrix element $[vw(J)-v'w'(J')]$ has the form

$$Z_1^{(\mathrm{RPA})}[vw(J)-v'w'(J')]\propto\sum_i\frac{Z_{nb}X_k(wnv'b)}{\epsilon_n+\epsilon_w-\epsilon_{v'}-\epsilon_b},$$

where the index b designates core states and n designates an excited state. For the special case of the $5d_{5/2}5d_{3/2}[2]$-$6p_{1/2}5d_{5/2}[1]$ transition, we obtain

$$Z_1^{(\mathrm{RPA})}[5d_{3/2}5d_{5/2}(2)-6p_{1/2}5d_{5/2}(3)]\propto\sum_n\sum_b\frac{Z(b,n)X_k(5d_{3/2}b6p_{1/2}n)}{\epsilon_n+\epsilon(5d_{3/2})-\epsilon(6p_{1/2})-\epsilon_b}.$$

In the case of $b=5p_{3/2}$ and $n=5d_{3/2}$ for nuclear charge $Z=88$, the denominator becomes

$$\epsilon(5d_{3/2})+\epsilon(5d_{3/2})-\epsilon(6p_{1/2})-\epsilon(5p_{3/2})=-0.278.$$

As before, the small value of the denominator leads to an anomalous increase in the size of the RPA matrix element.

[1] J. Sugar, J.-F. Wyart, G.J. van het Hof, and Y.N. Joshi, J. Opt. Soc. Am. B **11**, 2327 (1994).

[2] G.J. van het Hof, Y.N. Joshi, J.-F. Wyart, and J. Sugar, J. Res. Natl. Inst. Stand. Technol. **100**, 687 (1995).

[3] R.R. Kildiyarova, Y.N. Joshi, and J. Sugar, Phys. Scr. **53**, 560 (1996).

[4] R.R. Kildiyarova, Y.N. Joshi, S.S. Churilov, A.N. Ryabtsev, and J. Sugar, Phys. Scr. **55**, 438 (1997).

[5] S.S. Churilov, R. Gayasov, R.R. Kildiyarova, Y.N. Joshi, and A.N. Ryabtsev, Phys. Scr. **57**, 626 (1998).

[6] S.S. Churilov and Y.N. Joshi, Phys. Scr. **58**, 425 (1998).

[7] V.I. Azarov and S.S. Churilov, Opt. Spectrosc. **88**, 11 (2000).

[8] R.D. Cowan, *The Theory of Atomic Structure and Spectra* (University of California Press, Berkeley, 1981).

[9] S.G. Porsev, Y.G. Rakhlina, and M.G. Kozlov, Phys. Rev. A **60**, 2781 (1999).

[10] W.C. Martin, R. Zalubas, and L. Hagan, *Atomic Energy Levels—The Rare-Earth Elements* (U. S. GPO, Washington, DC, 1978).

[11] M.S. Safronova, W.R. Johnson, and U.I. Safronova, Phys. Rev. A **53**, 4036 (1996).

[12] W.R. Johnson, M.S. Safronova, and M.S. Safronova, Phys. Scr. **56**, 252 (1997).

[13] U.I. Safronova, W.R. Johnson, M.S. Safronova, and A. Derevianko, Phys. Scr. **59**, 286 (1999).

[14] U.I. Safronova, W.R. Johnson, and H.G. Berry, Phys. Rev. A **61**, 052503 (2000).

[15] U.I. Safronova, W.R. Johnson, D. Kato, and S. Ohtani, Phys. Rev. A **63**, 032518 (2001).

[16] P.F.A. Klinkenberg, T.A.M.V. Kleef, and P.E. Noorman, Physica (Amsterdam) **27**, 151 (1962).

[17] W.R. Johnson, S.A. Blundell, and J. Sapirstein, Phys. Rev. A **37**, 2764 (1988).

[18] M.H. Chen, K.T. Cheng, and W.R. Johnson, Phys. Rev. A **47**, 3692 (1993).

[19] I. Lindgren and J. Morrison, *Atomic Many-Body Theory*, 2nd ed. (Springer-Verlag, New York, 1986).

[20] U.I. Safronova, A. Derevianko, M.S. Safronova, and W.R. Johnson, J. Phys. B **32**, 3527 (1999).